CHAPTER

1

The Impacts of X-Ray Absorption Spectroscopy on Understanding Soil Processes and Reaction Mechanisms

Matthew Ginder-Vogel and Donald L. Sparks

Department of Plant and Soil Sciences, Delaware Environmental Institute,
University of Delaware, Newark, DE, USA

OUTLINE

1. INTRODUCTION AND INFORMATION GAINED FROM XAS

The determination of element speciation and distribution within heterogeneous environmental systems, such as soils, is crucial to developing a thorough understanding of soil processes and reaction mechanisms that control not only the transport of nutrients and contaminants, but also biomineralization and soil formation processes. The application of numerous spectroscopic and analytical techniques is required to solve these and other complex problems facing soil scientists. These techniques include X-ray absorption spectroscopy (XAS) (Brown et al., 1997a,b; Schulze and Bertsch, 1995; Sparks, 2005; Sparks and Borda, 2008), Fourier-transform infrared (FTIR) (Hind et al., 2001), Raman (Johnston and Wang, 2002), nuclear magnetic resonance (NMR) (Bleam, 1991), electron paramagnetic resonance (EPR) (Flogeac et al., 2004), and Mössbauer (Mc Cammon, 2004; Rancourt, 1998) spectroscopies. In addition, scanning and transmission electron microscopy (SEM and TEM), and atomic force microscopy (AFM) (Cail and Hochella, 2005; Hillner et al., 1992; Weaver and Hochella, 2003) complement these spectroscopic techniques.

During the last two decades, XAS has developed into a mature technique for obtaining the speciation (e.g., oxidation state) and short-range structure of elements present in heterogeneous soils and sediments (Fig. 1.1). XAS encompasses both X-ray absorption near-edge structure (XANES) spectroscopy and extended X-ray absorption fine structure (EXAFS) spectroscopy. XAS has a number of advantageous qualities for studying soils and sediments, which include elemental specificity, sensitivity to the local chemical and structural state of an element, and the ability to analyze materials *in situ* (Fig. 1.1). This information allows accurate determination of oxidation state, type of nearest neighbors, coordination number, bond distance, and orbital symmetries of the X-ray absorbing element. Fendorf (1999) and Kelly et al. (2008) provide a detailed discussion of applications of XAS to soil, clay, and environmental science and include summaries of the physical basis of XAS, experimental considerations, and data analysis techniques. Additionally, soil scientists have recently begun employing variations on traditional bulk XAS, including bulk and microfocused synchrotron X-ray diffraction (S-XRD and m-XRD, respectively), microfocused-XANES and EXAFS spectroscopies (m-XANES and m-EXAFS, respectively) (Brown and Sturchio, 2002) in addition to transmission or fluorescence tomography (Chapter 3) in the analysis of heterogeneous systems. X-ray fluorescence (XRF) mapping helps to determine the areas of interest to be analyzed in combination with m-XRD, m-XANES, and m-EXAFS (Fig. 1.1). Another variation is quick-scanning XAS, which allows the collection of a complete XANES or EXAFS spectrum in as little as 300 ms (Dent, 2002; Ginder-Vogel et al., 2009).

The previous decade has seen a rapid development in the number and variety of synchrotron user facilities at least partially dedicated to the soil and environmental sciences. In the United States, these facilities include, GeoSoilEnviroCARS (GeoSoilEnviroCARS, 2008), with beamlines located at both the Advanced Photon Source (APS) and the National Synchrotron Light Source (NSLS); Envirosuite (EnviroSuite, 2008), with beamlines located at the NSLS; and the Molecular Environmental Interface Science (MEIS) group (MEIS, 2008), located at the Stanford Synchrotron Radiation Laboratory (SSRL). Recently, several excellent reviews on the use of synchrotron techniques in environmental sciences have been published. These reviews focused on the use of synchrotron techniques in low-temperature geochemistry and environmental science (Fenter et al., 2002), clay and soil sciences (Schulze et al., 1999), interpretation of data collected from environmental systems (Kelly et al., 2008), and the study of heavy metals in the environment (Sparks, 2005). Additionally, recent journal

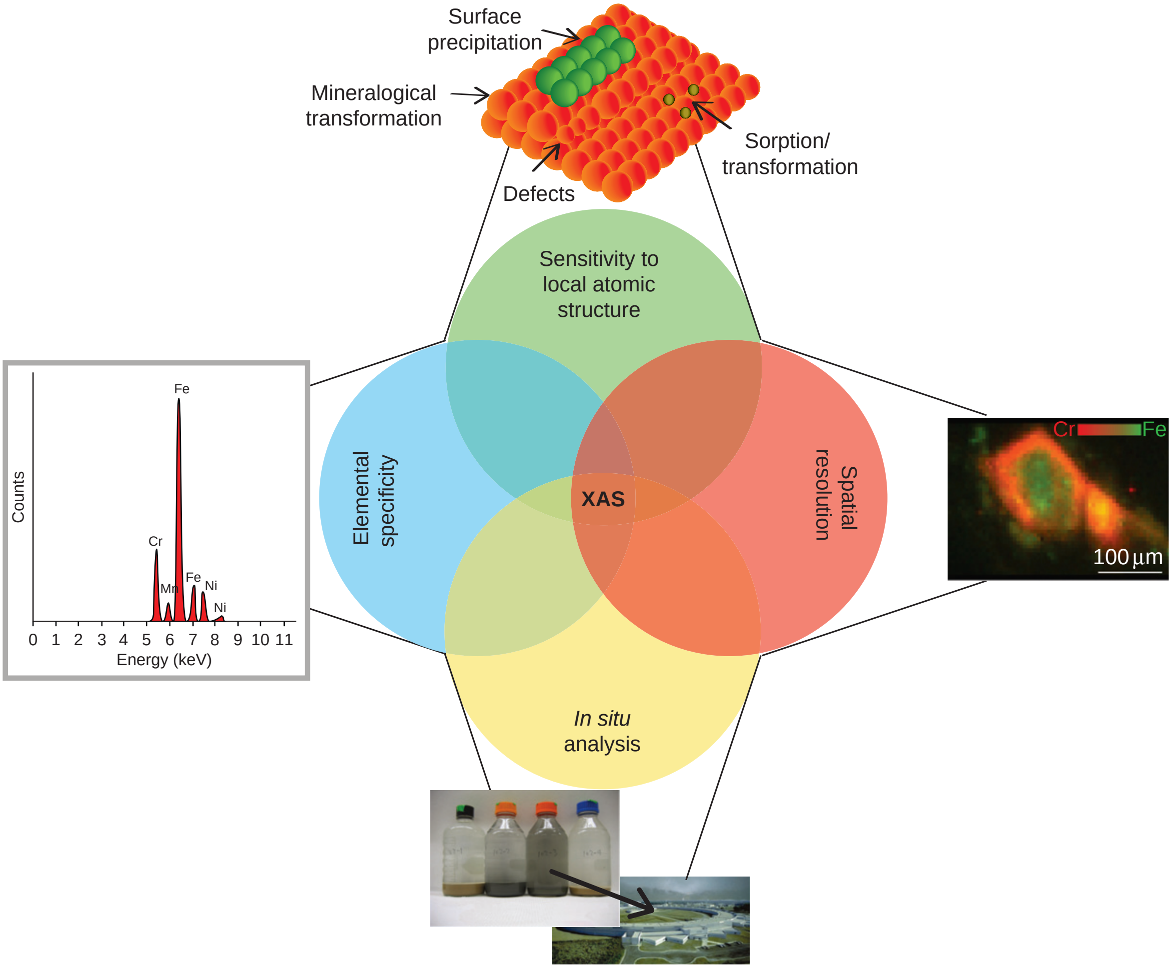

FIGURE 1.1 Advantageous characteristics of X-ray absorption spectroscopy (XAS) for analysis of heterogeneous soils and sediments.

issues on the impact of user facilities in environmental sciences have highlighted the critical importance of synchrotron research in soil science and related disciplines (Sutton, 2006). In this chapter, we will examine the application of a wide variety of synchrotron X-ray techniques to fundamental issues in environmental soil chemistry. However, first we provide a brief discussion of complementary spectroscopic and microscopic techniques that are often used in conjunction with XAS investigations.

2. COMPLEMENTARY/ ALTERNATIVE TECHNIQUES

Although XAS is a powerful analytical tool, it is best applied as one of several analytical techniques in order to obtain the clearest picture of the processes controlling elemental mobility in soil environments. In addition to the traditional analytical techniques used in soil chemistry, other advanced spectroscopic techniques are often used to complement the elementally specific data obtained from XAS.

2.1. Synchrotron X-Ray Diffraction

X-ray diffraction (XRD) is a fundamental technique used in the characterization and identification of crystalline materials in soils and sediments. Conventional XRD uses monochromatic X-rays generated when high voltage is applied to an anode, generally Cu. Conventional XRD is generally limited to crystalline materials; additionally, it is time consuming and often requires a relatively large sample volume. The low flux and relatively low energy of laboratory-based X-ray sources generally limits the geometry of the diffractometer, which requires data collection of diffracted X-rays, rather than transmitted X-rays, making analysis of hydrated or oxygen samples quite difficult. However, S-XRD offers exceptional resolution and sensitivity, even on very small samples. This permits the identification and quantification of trace phases, which is not possible using conventional X-ray sources. Additionally, amorphous materials, thin films, and hydrated samples can be analyzed due to the high flux of synchrotron X-ray sources and specialized instrumental configuration. With the use of area detectors or CCD cameras, similar to protein crystallography beamlines, it is possible to collect a single XRD pattern in a matter of seconds, allowing for *in situ*, real-time monitoring of aqueous reactions.

2.2. X-Ray Photoelectron Spectroscopy

X-ray photoelectron spectroscopy (XPS) uses X-rays to excite electrons from molecular orbitals into the continuum. However, rather than measuring X-ray absorption as a function of energy, XPS is conducted by using a fixed energy source to excite electrons from the sample and then measuring their kinetic energy. Since their kinetic energy is dependent on their binding energy, different chemical species can be identified. As with conventional XRD, these experiments are commonly carried out in laboratories, using Al or Mg anodes to produce monochromatic radiation. Since XPS measures electrons, it is highly surface sensitive, generally interrogating only the first few 100s of angstroms of a surface. Additionally, recent advances in synchrotron-based, ambient-pressure XPS measurements allow the measurement of hydrated samples (Ghosal et al., 2005).

2.3. Vibrational Spectroscopy (IR and Raman)

The first reported study of soil systems using vibrational spectroscopy is the study of water sorption to montmorillonite in 1937 (Buswell et al., 1937). Consequent to this study, the use of vibrational spectroscopies, such as infrared (IR) and Raman, have greatly contributed to our understanding of the structure, bonding, and reactivity of soil particles (Johnston and Wang, 2002). IR and Raman modes are very sensitive to small changes occurring in the local environment of the constituent atoms; therefore, these spectral perturbations may be used to gain insight into the interaction between absorbates and the particle surface. The recent development of attenuated total reflection Fourier-transform infrared (ATR-FTIR) methods has allowed the investigation of the particle solid-water interface under environmentally relevant (i.e., hydrated) conditions and has become one of the tools of choice to investigate the solid-liquid interface (Hind et al., 2001). Additionally, time-resolved ATR-FTIR can be used to follow the surface chemistry and determine kinetics of reactions occurring at mineral surfaces in real time (Parikh et al., 2008). The development of Raman microscopes has allowed Raman spectroscopy to be used to analyze spatially heterogeneous samples and is particularly useful in the analysis of organics and mineral phases (Johnston and

Wang, 2002). The fate and transport of pollutants, behavior of exchangeable cations in soils, bonding mechanism of pesticides, specific adsorption of anions, and the behavior of water near mineral surfaces are examples of research areas that have benefited from vibrational spectroscopy (Johnston and Wang, 2002). Vibrational spectroscopies are important tools used to investigate the mineral-water interface; however, they suffer from interferences from water, impurities, and the bulk solid itself (Johnston and Wang, 2002).

2.4. Mössbauer Spectroscopy

Mössbauer spectroscopy is a nuclear spectroscopy that has energy resolution sufficient to resolve the hyperfine structures of nuclear levels (Murad and Cashion, 2003; Rancourt, 1998). In a given experiment, it always operates on a single g-ray transition, the Mössbauer transition, between the ground state and an excited state of one isotope in the sample. Mössbauer spectroscopy probes the local electronic structure and, by extension, the local crystallographic, magnetic, and chemical environments. One of the primary limitations of its application to environmental systems is that the isotope of interest has a large enough recoilless fraction to exhibit measurable Mössbauer effects. To date, only 45 isotopes, including ^{57}Fe, have a large enough Mössbauer effect to be measurable. Other isotopes of interest to environmental scientists that may be measured via Mössbauer spectroscopy include ^{119}Sn, ^{151}Eu, ^{129}I, and ^{121}Sb. Another factor that may limit the application of Mössbauer spectroscopy to environmental systems is the complexity of interpreting the parameters controlling the relevant hyperfine interactions; spectral analysis often combines advanced data analysis and statistical methods with quantum mechanical and physical constraints in order to obtain a stable solution (Murad and Cashion, 2003). Nevertheless, Mössbauer spectroscopy has been extensively used in the study of Fe-bearing minerals in environmental settings. Recently, Williams and Scherer (2004) used Mössbauer spectroscopy to determine the reaction mechanism of Fe(II) sorption and oxidation at Fe(III) (hydr)oxide mineral surfaces. Many additional examples of the applications of Mössbauer spectroscopy are available in Murad and Cashion (2003).

2.5. Nuclear Magnetic Resonance and Electron Paramagnetic Resonance Spectroscopies

NMR and EPR spectroscopies have been important analytical tools in chemistry, material sciences, and organic geochemistry for several decades (Nanny et al., 1997); however, they have only recently become recognized as useful tools in the wider field of environmental science. NMR is a noninvasive probe that can be used to identify individual compounds and aids in determining structures of large macromolecules and examination of certain reaction kinetics. NMR spectroscopy measures the magnetic properties of NMR active nuclei (i.e., ^{1}H, ^{13}C, ^{15}N, ^{23}Al, ^{31}P, and ^{133}Cs) that are influenced not only by their chemical environments, but also by their physical interactions with their environments. Examination of environmentally relevant systems is significantly hampered by the low prevalence of most NMR active nuclei; however, with further developments in instrumentation, the sensitivity and utility of this technique is increasing. NMR has most frequently been applied to the study of soil organic matter; however, NMR has the potential to examine the pore size distribution (Chen et al., 2002b) as well as water flow and transport processes in soil (Chen et al., 2002a; Kinchesh et al., 2002).

EPR is a technique for studying chemical species that have one or more unpaired electrons. In soil science, it is generally applied to transition metals. Although the basic physical principles of

EPR are similar to those of NMR, the technique measures the relaxation of excited electron spins rather than excited nuclear spins. While EPR is less widely used than NMR, its ability to measure only paramagnetic species gives it tremendous elemental specificity, and EPR spectra can be recorded in just a few milliseconds, making it an ideal technique for measuring transition metal reaction kinetics. For example, Fendorf et al. (1993) studied Mn(II) sorption to birnessite on a time scale of milliseconds using stop-flow electron paramagnetic resonance (SF-EPR) spectroscopy.

2.6. Electron Microscopy

Scanning electron microscopy (SEM) and transmission electron microscopy (TEM) provide unique techniques to visually examine environmental samples. SEM is often used to examine the morphology of environmental particles >100 nm in size. Additionally, when coupled with energy dispersive spectroscopy (EDS), it allows mapping of major and minor elements on a scale of ~1 mm. TEM analysis can be used to examine much smaller features of soil particles, with high-resolution TEM (HR-TEM) providing a point-to-point resolution better than 1 Å. TEM is often coupled with EDS to provide elemental makeup. Selected area electron diffraction (SAED) can be used to identify crystalline materials on the nano-scale, while electron energy loss spectroscopy (EELS) is being used to identify elemental oxidation state on the nanometer scale. For example, Livi et al. (2009) used high-resolution TEM to confirm the amorphous nature of Ni layered double hydroxide (LDH) precipitates on pyrophyllite.

3. HISTORICAL ASPECTS OF XAS APPLICATIONS TO MINERAL/WATER INTERFACIAL REACTIONS

The employment of *in situ* (under natural conditions where water is present) molecular-scale techniques, such as synchrotron-based EXAFS and XANES spectroscopies, XRF, XRD, and microtomography, have been widely used over the past 20 years to study metal(loid) and radionuclide sorption phenomena at the mineral/water interface and to determine the chemical form (speciation) and distribution of environmental contaminants in heterogeneous natural materials, such as minerals and soils. Arguably, they have revolutionized many scientific fields, including soil science, geochemistry, and environmental sciences (Fig. 1.1).

Synchrotron light sources were first available to general users in 1974. The first published study that employed XAS to directly delineate the type of surface complexes formed at mineral/water interfaces was the seminal research of Hayes et al. (1987). Studying selenite and selenate sorption at the goethite/water interface, selenite was observed to primarily form an inner-sphere surface complex while selenate formed predominantly an outer-sphere complex. This was the first direct confirmation that inner- and outer-sphere surface complexes, first proposed by Werner Stumm and his co-workers, form on natural mineral surfaces. This study catalyzed a plethora of other studies over the next two decades, resulting in the active involvement by soil scientists in using synchrotron radiation techniques to study reaction mechanisms at mineral surfaces and speciation of inorganic contaminants in soils and biosolids. The growing use of these techniques, and their importance in addressing a multitude of environmental challenges involving soil, water, and air quality have resulted in the creation of a new multidisciplinary field referred to as *molecular environmental science*, which is the study of the chemical and physical forms and distribution of contaminants in soils, sediments, waste materials, natural waters, and the atmosphere at the molecular level.

4. APPLICATIONS OF XAS TO ELUCIDATE SOIL CHEMICAL PROCESSES AND REACTIONS

4.1. Adsorption of Metal(loids) on Soil Components

Since 1987, hundreds of studies using bulk XAS (Brown and Parks, 2001; Brown and Sturchio, 2002; Brown et al., 2006; Sparks, 1995, 2004c) have provided extensive information on metal and oxyanion sorption on metal hydr(oxides), phyllosilicates, humic substances, and other natural materials. This information includes structure, stoichiometry, attachment geometry (inner vs outer sphere, monodentate vs bidentate or tridentate), the presence of multinuclear complexes and precipitate phases, and the presence of ternary surface complexes, when complexing ligands are present in solution (Brown and Sturchio, 2002; Sparks, 2004c) (Table 1.1). The type of surface complexes on phyllosilicates and metal-(oxyhydr)oxides that occur with low atomic number metals, such as Al, B, Ca, Mg, S and Si, are not easy to ascertain using XAS under *in situ* conditions. However, major advances are being made in the area of soft X-ray spectroscopy that will enable direct determination of the types of surface complexes which form with these metals.

Based on molecular scale studies, including many using XAS, one can predict that alkaline earth cations, Mg^{2+}, Ca^{2+}, Sr^{2+} and Ba^{2+}, primarily form outer-sphere complexes while the divalent first-row transition metal cations, Mn^{2+}, Fe^{2+}, Co^{2+}, Ni^{2+}, Cu^{2+} and Zn^{2+}, and the divalent heavy metal cations such as Cd^{2+}, Hg^{2+} and Pb^{2+} primarily form inner-sphere complexes. At higher metal loadings and pHs, sorption of metals such as Co, Cr, Ni and Zn on phyllosilicates and metal-(hydr)oxides can result in the formation of surface precipitates (Fig. 1.1 and Table 1.1). The formation of these multinuclear and precipitate phases will be discussed in more detail later.

TABLE 1.1 Predominant sorption mechanisms for metals and metalloids on mineral surfaces

	Predominant Sorption Mechanism
Metals	
Cadmium	Inner-sphere
Cobalt	Inner-sphere (low loading), Co-Al hydroxide precipitates (high loading)
Chromium	Inner-sphere (low loading), Cr hydroxide precipitates (high loading)
Copper	Inner-sphere
Lead	Inner-sphere (low loading), Surface polymers (high loading)
Nickel	Inner-sphere (low loading), Ni-Al hydroxide precipitates (high loading)
Strontium	Outer-sphere
Zinc	Inner-sphere (low loading), Zn-Al hydroxide precipitates (high loading)
Metal(loids)	
Arsenite	Inner-sphere
Arsenate	Inner-sphere
Borate	Inner-sphere
Carbonate	Inner-sphere
Chromate	Inner-sphere
Phosphate	Inner-sphere
Selenate	Outer-sphere
Selenite	Inner-sphere
Sulfate	Outer-sphere

Note: These are the predominant sorption mechanisms that form on mineral surfaces based on surface spectroscopy (e.g., XAS and FTIR) studies. However, environmental factors such as pH, surface loading, time, and ionic strength can affect the type of surface complex and there may be multiple surface products that occur on a particular mineral. References for each metal(loid) can be found in Sparks (2002).

Although there are currently experimental limitations to using *in situ* molecular scale techniques to directly determine the type of surface complexes that the anions $NO_3{}^-$, Cl^- and ClO_4^-

form on mineral surfaces, one can propose that they are sorbed as outer-sphere complexes and sorbed on surfaces that exhibit a positive charge (Zhang and Sparks, 1990). Some researchers have also concluded that SO_4^{2-} (Zhang and Sparks, 1990) can be sorbed as an outer-sphere complex; however, there is other evidence that SO_4^{2-}may also sorb as an inner-sphere complex (Paul et al., 2007). There is direct spectroscopic evidence to show that selenate can sorb as both an outer-sphere and an inner-sphere complex depending on environmental factors (Hayes et al., 1987; Manceau and Charlet, 1994; Sparks, 2002, 2004a).

Most other anions such as molybdate, arsenate, arsenite, selenite, phosphate, and silicate appear to be strongly sorbed as inner-sphere complexes, and sorption occurs through a ligand exchange mechanism (Table 1.1). The sorption maximum is often not sensitive to ionic strength changes. Sorption of anions via ligand exchange results in a shift in the point of zero charge (pzc) of the sorbent to a more acid value (Sparks, 2002, 2004c).

Bulk XAS probes an area of several square millimeters and provides information on the local chemical environment of a surface. Thus, where more than one type of surface species is present, bulk XAS may detect only the primary (or average) type of surface product/species in the bulk sample (i.e., sums over all geometric configurations of the target atom). Consequently, while it may be concluded that the primary surface complex is inner-sphere, this does not necessarily mean that outer-sphere complexation is not occurring. Recently, through the use of X-ray scattering measurements to study metal(loid) binding on single crystal surfaces, Catalano et al. (2008) showed that arsenate surface complexation was bimodal, with adsorption occurring simultaneously as inner- and outer-sphere species. Environmental factors such as pH, surface loading, ionic strength, type of sorbent, and time also affect the type of sorption complex or product. An example of this is shown for Pb sorption on montmorillonite over an ionic strength (I) of 0.006-0.1 and a pH range of 4.48-6.77 (Table 1.2). Employing XAS analysis, at a pH of 4.48 and an *I* of 0.006, outer-sphere complexation on basal planes in the interlayer regions of the montmorillonite predominated. At a pH of 6.77 and *I* of 0.1, inner-sphere complexation on edge sites of montmorillonite was most prominent, and at pH of 6.76, *I* of 0.006 and pH of 6.31, *I* of 0.1, both inner- and outer-sphere complexation occurred. These data are consistent with other findings that inner-sphere complexation is favored at higher pH and ionic strength. Clearly, there is a continuum of

TABLE 1.2 Effect of *I* and pH on type of Pb adsorption complexes on montmorillonite

I (M)	pH	Removal from solution (%)	Adsorbed Pb(II) (mmol/kg)	Primary adsorption complex[a]
0.1	6.77	86.7	171	Inner sphere
0.1	6.31	71.2	140	Mixed
0.006	6.76	99.0	201	Mixed
0.006	6.40	98.5	200	Outer sphere
0.006	5.83	98.0	199	Outer sphere
0.006	4.48	96.8	197	Outer sphere

Source: Strawn and Sparks (1999), with permission.

[a] Based on results from XAFS data analysis.

adsorption complexes that can exist in soils (Sparks, 2002, 2004c).

4.2. Metal(loid) Surface Precipitation/ Dissolution

As the amount of metal cation or anion sorbed on a surface (surface coverage or loading that is affected by the pH at which sorption occurs) increases, sorption can proceed from mononuclear adsorption to surface precipitation (a three-dimensional phase) (Fig. 1.1 and Table 1.1). There are several types of surface precipitates that may arise via polymeric metal complexes (dimers, trimers, etc.) which form on mineral surfaces or via the sorption of aqueous polymers (Chisholm-Brause et al., 1990). Homogeneous precipitates often form on a surface when the solution becomes saturated and the surface acts as a nucleation site (Fig. 1.1). After adsorption attains monolayer coverage, it continues on the newly created sites, causing a precipitate on the surface (Chisholm-Brause et al., 1990; Farley et al., 1985; McBride, 1991; O'Day et al., 1994; Sposito, 1986). When the precipitate consists of chemical species derived from both the aqueous solution and dissolution of the mineral, it is referred to as a coprecipitate. The composition of the coprecipitate varies between that of the original solid and a pure precipitate of the sorbing metal. The ionic radius of the sorbing metal and sorbent ions must be similar for coprecipitates to form. Thus, Co(II), Mn(II), Ni(II), and Zn(II) (Chapter 8) form coprecipitates on sorbents containing Fe (III), Al(III), and Si(IV) and possibly Pb(II), which is considerably larger (1.20 Å). Coprecipitate formation is generally limited by the rate of mineral dissolution, rather than the lack of thermodynamic favorability (McBride, 1994; Scheidegger et al., 1998). If the formation of a precipitate occurs under solution conditions that would, in the absence of a sorbent, be undersaturated with respect to any known solid phase, this is referred to as surface-induced precipitation (Sparks, 2004c; Sparks and Borda, 2008; Towle et al., 1997).

Thus there is often a continuum between surface complexation (adsorption) and surface precipitation. At low surface coverage, surface complexation (e.g., outer- and inner-sphere adsorption) tends to dominate. As surface loadings increase, nucleation occurs and results in the formation of distinct entities or aggregates on the surface. As surface loadings increase further, surface precipitation becomes the dominant mechanism.

Using *in situ* bulk XAS, it has been shown by a number of scientists that multinuclear metal hydroxide complexes and surface precipitates Co(II), Cr(III), Cu(II), Ni(II) and Pb(II) can form on metal oxides, phyllosilicates, soil clays and soils (Bargar et al., 1995; Charlet and Manceau, 1992; Chisholm-Brause et al., 1990, 1994; Elzinga and Sparks, 1999; Fendorf et al., 1994; Ford and Sparks, 2000; O'Day et al., 1994; Papelis and Hayes, 1996; Roberts et al., 1999; Roe et al., 1991; Scheckel and Sparks, 2001; Scheidegger et al., 1996a,b, 1997, 1998; Thompson et al., 1999a,b; Towle et al., 1997). These metal hydroxide phases occur at metal loadings below a theoretical monolayer coverage and in a pH range well below the pH where the formation of metal hydroxide precipitates would be expected, according to the thermodynamic solubility product (Scheidegger and Sparks, 1996; Sparks, 2002, 2004b; Sparks and Borda, 2008).

Scheidegger et al. (1997) were the first to show that sorption of metals, such as Ni, on an array of phyllosilicates and Al oxide can result in the formation of mixed metal-Al hydroxide surface precipitates, which appear to be coprecipitates. The precipitated phase shares structural features common to the hydrotalcite group of minerals and the layered double hydroxides (LDH) observed in catalyst synthesis. The LDH structure is built of stacked sheets of edge-sharing metal octahedra, containing divalent and trivalent metal cations separated by anions between the interlayer

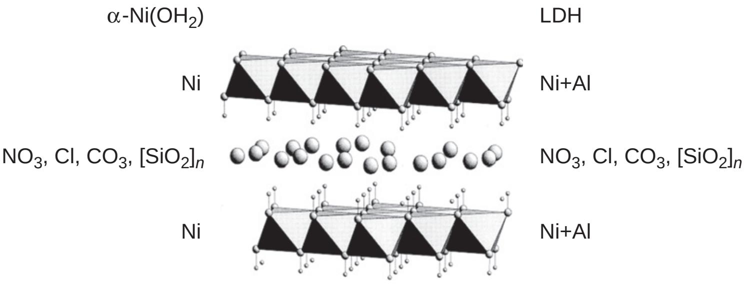

FIGURE 1.2 Structure of Ni-Al layer double hydroxide (LDH) showing brucite-like octahedral layers in which Al^{3+} substitutes for Ni^{2+} creating a net positive charge that is balanced by hydrated anions in the interlayer space (Ford et al., 1999).

spaces (Fig. 1.2). The general structural formula can be expressed as $[Me^{2+}_{1-x} Me^{3+}_{x} (OH)_2]^{x+} \cdot (x/n) A^{n}$-$mH_2O$, where for example, Me^{2+}could be Mg (II), Ni(II), Co(II), Zn(II), or Mn(II), and Fe(II) and Me^{3+} could be Al(III), Fe(III), and Cr(III) (Towle et al., 1997). The LDH structure exhibits a net positive charge per formula unit, which is balanced by an equal negative charge from interlayer anions A^{n-}, such as Cl^-, Br^-, I^-, NO_3^-, OH^-, ClO_4^-, and CO_3^{2-}; water molecules occupy the remaining interlayer space (Allmann, 1970; Taylor, 1984). The minerals takovite, $Ni_6Al_2(OH)_{16}CO_3{\cdot}H_2O$ and hydrotalcite, $Mg_6Al_2(OH)_{16}CO_3{\cdot}H_2O$ are among the most common natural mixed-cation hydroxide compounds containing Al (Sparks, 2004b; Sparks and Borda, 2008; Taylor, 1984). Recently, Livi et al. (2009), using an array of microscopic techniques including analytical electron microscopy (AEM), high-resolution transmission electron microscopy (HR-TEM), and powder XRD, conducted studies to elucidate the nature of Ni hydroxide precipitates, using the same environmental conditions employed by Scheidegger et al. (1997) and reaction times ranging from 1 h to 5 years. While the precipitate phase had a bonding environment like a Ni-Al LDH, the precipitate was amorphous.

Mixed Co-Al and Zn-Al hydroxide surface precipitates also can form on aluminum-bearing metal oxides and phyllosilicates (Ford and Sparks, 2000; Thompson et al., 1999a,b; Towle et al., 1997). This is not surprising as Co^{2+}, Zn^{2+}, and Ni^{2+} all have ionic radii similar to Al^{3+}, enhancing substitution in the mineral structure and formation of a coprecipitate. However, surface precipitates have not been observed with Pb^{2+}, as Pb^{2+} is too large to substitute for Al^{3+} in mineral structures (Sparks, 2002, 2004c; Sparks and Borda, 2008).

The mechanism for the formation of metal hydroxide surface precipitates is not clearly understood. It is clear that the type of metal ion determines whether metal hydroxide surface precipitates form, and the type of surface precipitate formed, that is, metal hydroxide or mixed metal hydroxide is dependent on the sorbent type. Additionally, the reaction pH, which controls the degree of metal loading, is a major factor in determining the formation of metal hydroxide precipitates: for example below pH 6.5, metal hydroxide precipitates generally do not form on mineral surfaces or in soils (Elzinga and Sparks, 1999, 2001; Roberts et al., 1999, 2003).

The formation of metal hydroxide surface precipitates is an important mechanism of metal sequestration. As the surface precipitates age, metal release is greatly reduced (Fig. 1.3). Thus, the metals are less prone to leaching and less bioavailable to plants and microbes. Peltier et al. (2010) reacted three soils of varying mineralogy and organic matter content with 3 mM Ni at two pHs, 6 and 7.5, and evaluated Ni bioavailability using a biosensor. At pH 6, surface precipitates did not form and most of the Ni was bioavailable. However, at pH 7.5, where precipitates were observed to form from XAS analyses, Ni bioavailability is markedly reduced.

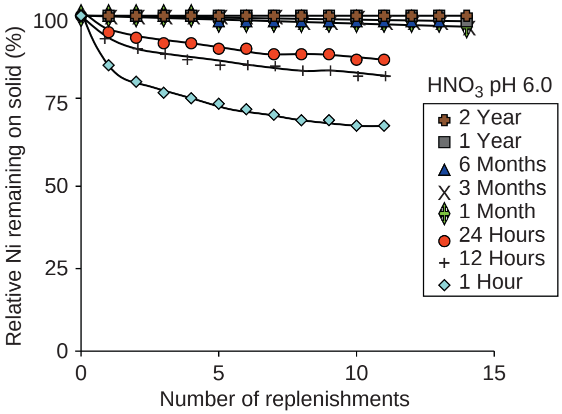

FIGURE 1.3 Dissolution of Ni from surface precipitates formed on pyrophyllite at residence times of 1 h to 2 years. The figure shows the relative amount of Ni^{2+} remaining on the pyrophyllite surface following extraction for 24 h periods (each replenishment represents a 24 h extraction) with HNO_3 at pH 6.0.

The decrease in metal release and bioavailability is linked to the increasing silication of the interlayer of the LDH phases with increased residence time, resulting in a mineral transformation from a LDH phase to a precursor phyllosilicate surface precipitate (Ford and Sparks, 2000; Ford et al., 1999). The mechanism for this transformation is thought to be due to diffusion of Si, originating from weathering of the sorbent, into the interlayer space of the LDH, replacing the anions such as NO_3^-. Polymerization and condensation of the interlayer Si slowly transforms the LDH into a precursor metal-Al phyllosilicate. The metal stabilization that occurs in surface precipitates on Al-free sorbents (e.g., talc) may be due to Ostwald ripening, resulting in increased crystallization; however, as noted earlier, microscopic analyses have shown that Ni-Al LDH phases appear to be amorphous (Livi et al., 2009). Using acid-solution calorimetry and results from previous calorimetry studies, Peltier et al. (2006) demonstrated that the enthalpy of formation of LDH phases is more exothermic, indicating greater stability, in order of $Cl<NO_3<SO_4<CO_3<Si$ of interlayer anionic composition, and that LDH phases were much more stable than a $Ni(OH)_2$ phase.

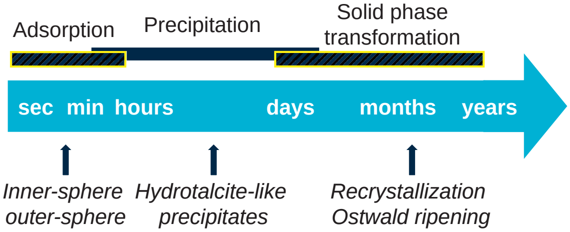

FIGURE 1.4 Changes in sorption processes with time showing a continuum from adsorption to precipitation to solid phase transformation (Sparks, 2002).

In short, with time, one sees that metal sorption on soil minerals can often result in a continuum of processes, from adsorption to precipitation to solid-phase transformation (Fig. 1.4), particularly in the case of certain metals, such as Co, Ni, and Zn. The formation of metal surface precipitates could be an important mechanism for sequestering metals in soils, such that they are less mobile and bioavailable. Such products must be considered when modeling the fate and mobility of metals like Co^{2+}, Mn^{2+}, Ni^{2+} and Zn^{2+} in soil and water environments (Sparks, 2002, 2004c; Sparks and Borda, 2008).

4.3. Redox Reactions on Soil Components

The mobility and environmental threat of many contaminants and nutrients is determined in large part by their redox state and the redox conditions of the soil environments in which they exist. XAS is an ideal tool for determining the oxidation states of elements in complex environmental media such as soils and sediments. Changes in oxidation state of an element result in a change in the energy required to excite core electron into the continuum, which manifests itself by a shift in the half-height position of the absorption edge for an element and can be determined using

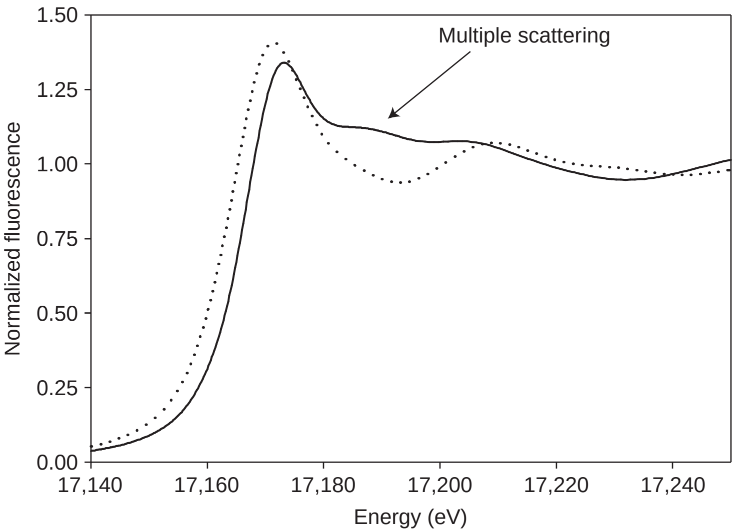

FIGURE 1.5 Uranium L_{III}-edge XANES spectra of uraninite (dotted) and uranyl nitrate hexahydrate (solid). The arrow indicates the contribution of multiple scattering from the uranyl moiety.

XANES spectroscopy. In addition, a change in the element's local coordination environment occurs and is manifested in EXAFS spectra of the element. This is readily exemplified by the reduction of soluble $U(VI)O_2^{2+}$ (and its various complexes) to $U(IV)O_2$, which results in the absorption edge shifting ~3 eV lower in energy (Fig. 1.5). Additionally, the transition from the highly linear uranyl ion results in the loss of a large shoulder, due to multiple scattering, that immediately follows the white line (Fig. 1.5) (Kelly et al., 2002, 2007, 2008). Further applications of XAS to environmental uranium (U) chemistry are described in detail by Kelly in Chapter 14 in this book.

In addition to U, XAS has been used to investigate metal and oxyanion cycling in many redox active systems (Bank et al., 2007; Bostick et al., 2002; Fendorf et al., 1992, 2002; Ginder-Vogel and Fendorf, 2008; Hansel et al., 2003a, 2005; Manning et al., 2002; Webb et al., 2005a,b;). The primary elements of interest include environmentally predominant transition metals, such as Fe and Mn, in addition to elements that exist in the environment primarily as oxyanions, such as As, Cr, and Se. Many of these redox reactions are driven by bacterial metabolism and result in the formation of hydrated mineral phases, making *in situ* (i.e., wet) analysis critical to determining the operative redox pathways.

4.3.1. *Transition Metal Oxides*

The environmental prevalence of iron and manganese oxides, hydroxides, and oxyhydroxides [(hydr)oxides], coupled with the large quantity of their highly reactive surface area, make them an important pool of reactivity, with regard to contaminant and nutrient absorption and redox transformation. However, their reactivity, in terms of both sorption and redox chemistry, is radically altered by changes in redox conditions, especially as they impact the mineralogy and surface chemistry of Fe and Mn (hydr)oxide phases.

Ferrihydrite, a poorly crystalline Fe(III) (hydr)oxide, is often found in soils and sediments that oscillate between reducing and oxidizing conditions. Due to its high surface area and intrinsic reactivity, ferrihydrite serves as a critical sink for contaminants (e.g., As and U) and nutrients (e.g., P); however, until recently, the impact of reducing conditions on the evolution of Fe(III) mineral mineralogy and its subsequent ability to retain and interact with contaminants and nutrients have been poorly understood. XAS, coupled with other advanced analytical techniques, has played a key role in furthering our understanding of this important environmental process. Ferrihydrite is considered the most bioavailable Fe(III) (hydr)oxide for dissimilatory metal reducing bacteria, which couple the oxidation of organic matter and H_2 to the reduction of Fe(III) and are ubiquitous in saturated soils and sediments. Upon dissimilatory metal reduction, the production of Fe(II) may result either in Fe(III) mineral dissolution or the rapid transformation of poorly crystalline Fe(III) (hydr)oxides into more crystalline and/or mixed Fe(II)/Fe(III) (hydr)oxides, depending on the intensity of Fe(III) reduction. The application of XAS to the study of Fe oxides is discussed in more detail in Chapter 8.

XAS has played a vital role in the identification and quantification of Fe (hydr)oxide mineralogy. In batch experiments using ferrihydrite, the solid phases formed during microbial iron reduction are dominated by the metabolic byproducts of Fe reduction, including ferrous iron and bicarbonate; and generated minerals are rich in Fe(II) and bicarbonate, including siderite, green rusts, and magnetite (Fredrickson et al., 1998; Liu et al., 2001). In general, this type of concentrated batch reaction produced high enough concentrations of the products of biological Fe reduction to be detected using traditional techniques, such as laboratory-based XRD and Mössbauer spectroscopy. However, in order to investigate the transformation of Fe (hydr)oxide minerals under more natural conditions, Fendorf and co-workers (Hansel et al., 2003a, 2005; Kocar et al., 2006; Nico et al., 2010) transitioned to Fe oxide-coated sand, which was packed into columns. This allowed Fe biomineralization to be studied under conditions that transported microbial metabolites away from the reaction site. Although a variety of analytical methods were used to analyze the resultant Fe mineralogy, including SEM, HR-TEM, XRD, and Mössbauer spectroscopy, they found that the most accurate and quickest method that allowed the quantification of the various iron mineral phases was EXAFS spectroscopy combined with linear combination analysis (Hansel et al., 2003a, 2005). Using this technique, Hansel et al. (2005) demonstrated that the mineralogical transformation of Fe(III) (hydr)oxides is dependent on the Fe(III) flux resulting from microbial iron reduction. At high Fe(II) concentrations, the dominant mineralogical products include magnetite and goethite, while lepidocrocite and goethite were observed at lower Fe(II) concentrations. Interestingly, more reduced phases, such as green rusts and Fe(II)-bearing minerals, were not observed in any experiments where flow conditions were used. This pioneering work has formed the basis for a series of studies that examine the effect of microbial iron reduction on the incorporation of other metals and metalloids, such as U and Cr, into iron oxide mineral structures during biological Fe reduction and abiotic redox reactions.

Widespread U contamination is present throughout the world as a result of natural U deposits, mining activities, and nuclear weapons and fuel production. Environmental U speciation is dominated by two oxidation states with markedly different properties. U(VI), as the uranyl cation (UO_2^{2+}), is thermodynamically stable under oxidizing conditions and is highly soluble in the presence of dissolved bicarbonate. Although uranyl sorption to solids such as Fe (hydr)oxides may be appreciable, it is largely reversible and is thus subject to changes in aqueous conditions and Fe (hydr)oxide mineralogy. Dissolved U can be reduced through the transformation of U(VI) into U(IV), forming the solid uraninite (UO_2), which is sparingly soluble under most environmental conditions. However, UO_2 may be reoxidized, thereby releasing U, by many oxidants including O_2, NO_3^-, Mn

(IV) oxides, and Fe(III) (hydr)oxides (Ginder-Vogel and Fendorf, 2008). Given the prevalence of Fe (hydr)oxide minerals in the environment and their critical role in controlling U mobility, much research has focused on the interaction of U complexes with iron, particularly as (hydr)oxide mineral phases as discussed by Kelly in Chapter 14 of the book. However, we have only recently begun to understand the role of iron (hydr)oxides in catalyzing uraninite oxidation and incorporation of U into the Fe (hydr)oxide mineral structure. Ginder-Vogel et al. (2006) and Ginder-Vogel and Fendorf (2008) used a combination of S-XRD and XAS to identify and quantify Fe oxide minerals produced during the oxidation of biologically precipitated uraninite by ferrihydrite. This work revealed that ferrihydrite is capable of oxidizing biogenic uraninite; however, the oxidation reaction is ultimately limited by the conversion of ferrihydrite into more thermodynamically stable forms, such as lepidocrocite and goethite (Fig. 1.6). Interestingly, during Fe(II) catalyzed ferrihydrite remineralization, U(VI) is substituted for between 3% and 6% of iron sites in transformation products (Nico et al., 2010). The substituted U is stabile even in the presence of strongly complexing solutions (30 mM $KHCO_3$) and during redox cycling (Stewart et al., 2009) and can be environmentally important as a long-term U sink.

Similar to U, Cr predominantly exists in the environment in two oxidation states, Cr(III) or Cr(VI). Chromium(VI), chromate, is highly toxic to humans and is quite soluble and hence mobile under most common environmental conditions. Conversely, Cr(III) is less toxic and generally immobile. There are many abiotic and biotic pathways of Cr reduction in the environment; however, under neutrophilic conditions, kinetic considerations favor Cr(VI) reduction by either dissolved Fe(II) or Fe(II)-bearing mineral phases (Fendorf et al., 2002). The identification and quantification of Cr oxidation states, using XANES spectroscopy, is quite straightforward due to a prominent pre-edge peak at 5993 eV, when Cr is present as Cr(VI) (Peterson et al., 1996, 1997), which is caused by a bound-state 1s to 3d transition. This transition is forbidden for centrosymmetric, octahedral $Cr(III)O_6$, but allowed for the noncentrosymmetric, tetrahedrally coordinated $Cr(VI)O_4$ molecule due to mixing of the Cr(3d) and O(2p) orbitals. The intensity of this pre-edge

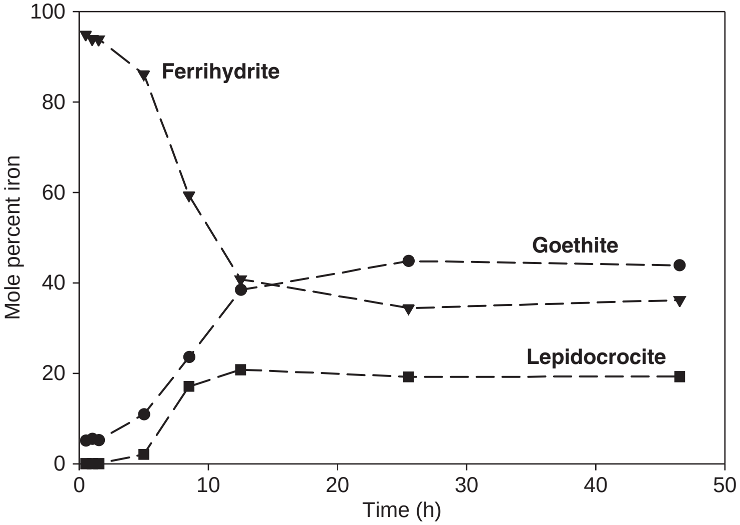

FIGURE 1.6 Transformation of ferrihydrite by Fe(II) generated during uraninite oxidation. Reactions were conducted with 3.0 mM $KHCO_3$, 30.7 m^2/L UO_2, and 23.5 m^2/L mM-Fe as ferrihydrite in 3 mM HCO_3^- at pH 7.2. Percentages (±5%) were determined from linear combination fits of k^3-weighted Fe EXAFS spectra (k = 1-14) (Ginder-Vogel et al., 2010).

feature can be used to quantify the proportion of Cr(VI) in a sample, at Cr(VI) concentrations $>$1-5%. Using this technique, several studies have examined Cr speciation in reducing, Cr-contaminated soils (Bank et al., 2007; Fendorf and Zasoski, 1992; Kendelewicz et al., 2000; Patterson et al., 1997;) and determined that less mobile Cr(III) was the dominant species in these systems; however, this may not always be the case in oxic systems. Using a combination of bulk XAS, m-XRF, and m-XRD to analyze sediments from the arid, oxic, Cr-contaminated Hanford site in Eastern Washington state, in conjunction with flow-through column experiments, Ginder-Vogel et al. (2005) identified several Fe(II)-bearing phyllosilicate minerals as the primary reductants of Cr(VI) in these sediments. However, depending on geochemical conditions, as much as 50% of the solid-phase Cr remained in the hexavalent form.

In large part, the solubility of Cr(III) that is abiotically reduced by Fe(II) is determined in large part by the ratio of Cr(III) to Fe(III) in the (hydr)oxide precipitate of the general formula $Fe_xCr_{1-x}(OH)_3$ (Sass and Rai, 1987). The solubility of Cr(III)-hydroxide precipitates is proportional to the ratio of Cr(III) to Fe(III), with increased quantities of Fe(III) stabilizing the solid (Sass and Rai, 1987). Generally, the ratio of Cr to Fe in hydroxide solids is determined using *ex situ* extraction methods, which may be compromised by Fe contamination of environmental samples; however, EXAFS spectroscopy presents an alternative method for determining this molar ratio (Hansel et al., 2003b). The intensity of the corner-sharing peak at 3.48-3.56 Å, normalized to the first Cr-Cr(Fe) shell, has a linear relationship with the mole fraction of Cr(III) within a mixed Cr(III)-Fe(III) solid.

4.4. Speciation of Soil Contaminants

With the advent of third-generation synchrotron light sources that have higher flux and higher brightness X-rays, together with state-of-the-art detectors and improved beamline optics, microfocused beams for spectromicroscopy and imaging are available to study heterogeneous natural systems such as soils, biosolids, and plants. With these techniques, it is possible to study areas of 1 mm^2 and focus the beam to spatial resolutions of <5 mm, enabling direct speciation of contaminants in heterogeneous materials. This has been a major advance in the past 10 years, and coupled with microfocused XRF, one can also determine the distribution and association of metals and oxyanions in complex natural systems. While bulk XAS can and should be used to determine the major species that are found in such systems, one needs to couple these studies with m-XAS and XRF investigations. There are several disadvantages in using bulk XAS to speciate contaminants in heterogeneous systems such as soils. Soils are complex and contain an array of inorganic and organic components, including humic substances, phyllosilicates, metal hydr(oxides), macro- and micropores, and microorganisms, all closely associated with each other. In such systems, some microenvironments contain isolated phases in higher concentrations relative to the average in the total (bulk) matrix. For example, the oxides, phyllosilicates, and microorganisms in the rhizosphere have quite a different chemical environment as compared to the bulk soil. These phases may be very reactive and important in the partitioning of metals, but may be overlooked using other analytical techniques that measure the average of all phases. In systems where more than one type of surface species is present, bulk XAS will detect only the primary (or average) type of surface product/species in the bulk sample. However, the most reactive sites in soils generally have particle sizes in the micrometer range, and metal speciation may vary over regions of a few 100 mm^2. The existence of multiple species in soils results in overlapping atomic shells and it is difficult to ascertain the precise metal speciation with bulk XAS.

Minor metal-bearing phases, even though they may constitute the most reactive or significant species, may not be successfully detected with bulk analyses (McNear et al., 2005).

Some excellent reviews have appeared on the application of m-XAS and XRF to speciate contaminants in heterogeneous systems (Bertsch and Hunter, 1998; Bertsch and Seaman, 1999; Hunter and Bertsch, 1998; Manceau et al., 2003). A number of investigations have appeared over the past 10 years on the speciation of metals and oxyanions, soils, plants, biosolids, and fly ash (see references in Brown and Sturchio, 2002).

4.4.1. *Microscale Speciation of Metal(loids)*

Some examples of studies that have used m-XAS and XRD to speciate metal(loids) in soils include those by Hunter and Bertsch (1998), Manceau et al. (2000), Isaure et al. (2002), Strawn et al. (2002), Roberts et al. (2005), Ginder-Vogel et al. (2005), Nachtegaal et al. (2005), Arai et al. (2006), McNear et al. (2007), and Grafe et al. (2008). A few examples of these studies will be summarized below. Additional details on m-XAS applications and data analyses methods for heterogeneous systems can be found in Manceau et al. (2000), Bertsch and Hunter (2001) and Chapter 2.

Nachtegaal et al. (2005) investigated the speciation of Zn in smelter contaminated soils from a large site in Belgium in which part of the site had been remediated by adding beringite, an aluminosilicate material, compost, and planting metal-tolerant plants. The other portion of the site was not treated. The objectives of the study were to determine how Zn speciation differed in the remediated and nonremediated soils. Specifically, the study sought to determine if Zn-LDH phases were present in the soils, and the stability of the Zn under different environmental conditions.

In the study of Nachtegaal et al. (2005), both mineral (e.g., willemite, hemimorphite, spalerite) and sorbed (Zn-LDH) Zn species predominated. The speciation differences in the remediated and nonremediated soils were slight, with the major difference being the presence of kerolite, a Zn phyllosilicate phase, found in the remediated site (Fig. 1.7). Desorption studies, using both $CaCl_2$ and HNO_3 at pH 4 and 6, showed that the Zn in both remediated and nonremediated soils was quite stable, reflecting again the role that metal surface precipitates, that is, Zn-LDH phases, play in sequestering metals such that mobility and bioavailability are diminished.

Grafe et al. (2008) used m-XRF and m-XAS to study the speciation of As in a chromated-copper-arsenate (CCA) contaminated soil to determine the effects of co-contaminating metal cations (Cu, Zn, Cr) on As speciation. Data analyses revealed that As occurred as a continuum of fully and poorly ordered copper-arsenate precipitates (63-75% of As species) and surface adsorption complexes on goethite and gibbsite in the presence and absence of structural Zn. Other non-Cu-based precipitates such as scorodite, adamite, and ojuelaite were also found. These data point out that association of As with Cu suggest that the speciation of As in a contaminated soil is not entirely controlled by surface adsorption reactions, but influenced significantly by the co-contaminating metal cation fraction.

4.4.2. *Speciation of Nutrients in Soils and Biosolids*

A number of studies have used particularly XANES to speciate nutrients such as P in soils and biosolids (see references cited in Chapter 11). Hesterberg et al. (1999) used XANES to investigate adsorbed and mineral phases of phosphate on Al and Fe oxides. They also showed that the predominant phase of phosphate in a North Carolina soil sample was dicalcium phosphate. Peak et al. (2002) investigated the speciation of P in alum-amended and nonamended poultry litter samples using XANES. Alum is used in the poultry industry

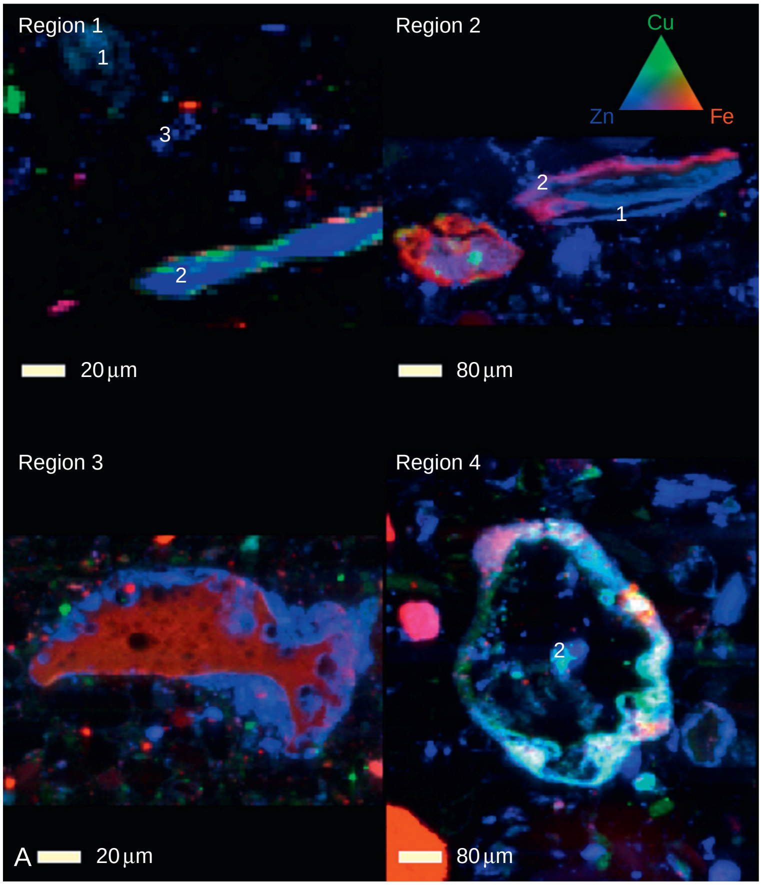

FIGURE 1.7 (A) m-SXRF tricolor maps for the treated soil samples. The numbers indicate the spots where m-EXAFS spectra were collected.

Continued

to reduce the level of water soluble P in litter before it is land applied. In the unamended litter, the predominant P species were a mixture of aqueous phosphate, organic phosphate, and dicalcium phosphate. In the alum-amended litter samples, the major species were P adsorbed on Al-oxides, organic phosphate, and aqueous phosphate. These results indicate that the addition of alum reduces the mobility of P in the litter material. There was no evidence of Al phosphate precipitates being present in the alum-amended samples. However, such phases could have occurred immediately after alum was added when the pH is low, *ca.* 5, but increases with time to *ca.* 7. With the rise in pH, any initial Al phosphate precipitates would undergo dissolution. XANES, along with more detailed speciation analyses, including linear combination fitting, was used in several studies (Beauchemin et al., 2003; Seiter et al., 2008; Shober et al., 2006; Toor et al., 2005) to more quantitatively speciate P in soils, turkey manures, and poultry litter. In order to get a better assessment of organic P species, which are known to be significant in poultry litter, Seiter et al. (2008) used principal

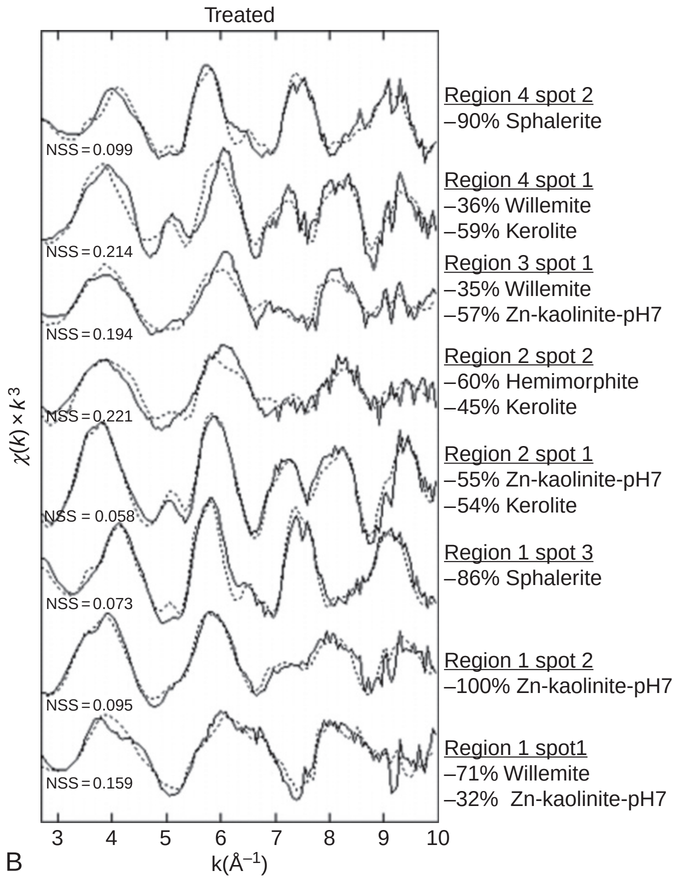

FIGURE 1.7—Cont'd (B) m-EXAFS spectra from selected spots on thin sections from the treated soil.

Continued

component analysis, target transformation, and linear least squares fitting to assess P speciation in alum-amended and nonamended poultry litter samples. They found that alum-amended poultry litter contained higher amounts of Al-bound P and phytic acid, whereas nonamended samples contained Ca-P minerals and organic P compounds.

4.4.3. *Coupling Kinetic Measurements with Molecular Scale Techniques in Real Time*

In soil environments, chemical reactions at the mineral/water interface occur over a range of temporal scales, ranging from microseconds to years. Many important processes (e.g., adsorption, oxidation-reduction, precipitation) occurring at mineral surfaces are characterized by a rapid initial reaction on time scales of milliseconds to minutes (Scheidegger and Sparks, 1996). Knowledge of these initial reaction rates is critical to determining chemical kinetic rate constants and reaction mechanisms, both of which are necessary to understand environmental chemical processes. Kinetic measurements, using traditional techniques, such as batch or stirred-flow techniques, typically yield only a few data points during the initial phases of the reaction and cannot

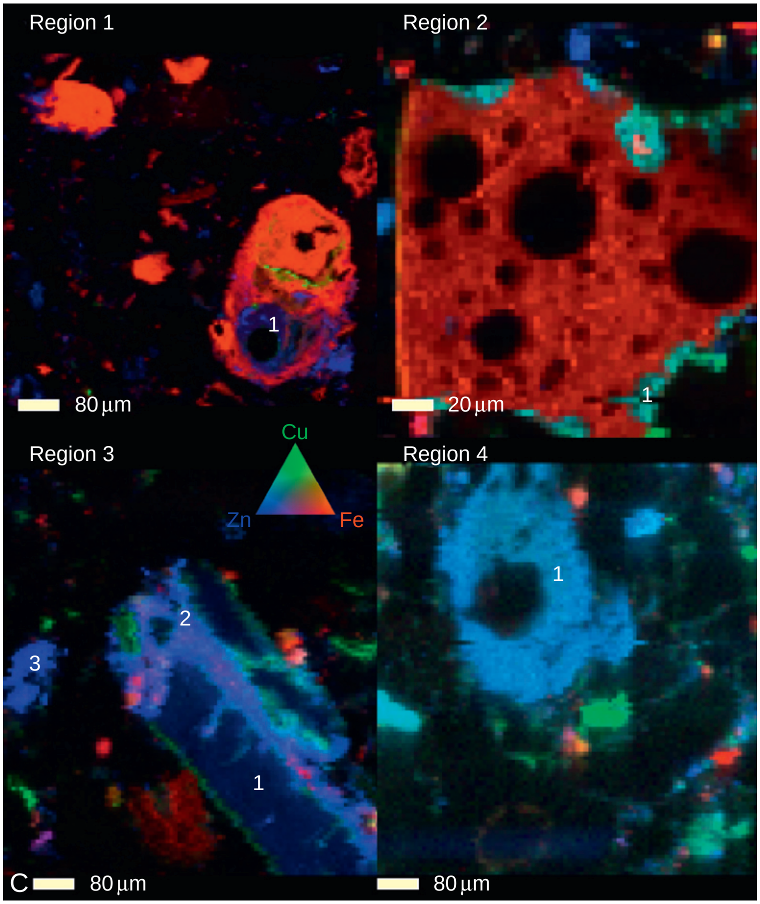

FIGURE 1.7—Cont'd (C) m-SXRF tricolor maps for the nontreated soil samples.

Continued

capture important reaction rates on second and slower time scales. Chemical relaxation techniques such as pressure jump (p-jump) and concentration jump (c-jump such as stopped-flow) allow rapid data collection on time scales of milliseconds. However, rate "constants" are calculated from linearized rate equations that include parameters that were determined from equilibrium and modeling studies. Consequently, the rate "constants" are not directly determined.

Direct, *in situ*, molecular scale measurement of rapid reactions has, until recently, been quite limited. Fendorf et al. (1993) used SF-EPR spectroscopy to measure Mn(II) sorption to birnessite (d-MnO$_2$) on a time scale of milliseconds. More recently, Parikh et al. (2008) used *in situ*, ATR-FTIR spectroscopy to measure As(III) oxidation rates by hydrous manganese(IV) oxide (HMO) at a time scale of ∼2.5 s. However, both of these techniques suffer from significant limitations. EPR can only be used to measure EPR-active nuclei, while FTIR requires both IR-active functional groups and relatively high concentrations of the reactants being examined (Parikh et al., 2008).

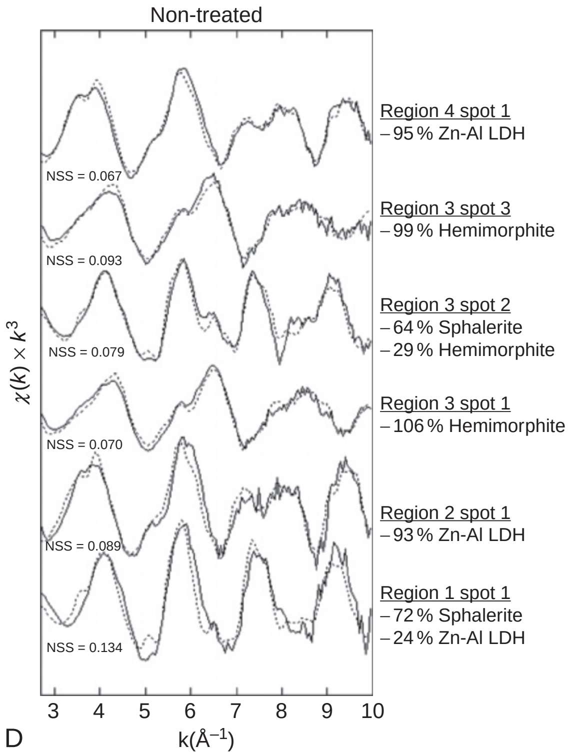

FIGURE 1.7—Cont'd (D) m-EXAFS spectra from selected spots on thin sections from the nontreated soil. The solid line indicates the raw $k^3 \times$ chi(k) data and the dotted line indicates the best fits obtained with linear combination fitting (Nachtegaal et al., 2005).

Quick-scanning X-ray absorption spectroscopy (QXAS) overcomes both of these limitations. Depending on beamline instrumentation and flux, QXAS can be used to probe most of the atoms on the periodic table and to relatively low concentrations (Khalid et al., 2010). The majority of the quick-scanning beamlines in the world collect a complete EXAFS scan in ~1 min, by slewing the monochromator from low energy to high energy and repeating the process (Mitsunobu et al., 2006). An alternative method for rapidly collecting EXAFS data is to perform energy-dispersive measurements; however, this technique generally suffers from poor sensitivity (Dent, 2002). However, using a unique, cam-operated, continuous-scanning setup at beamline X18B at the NSLS, it is possible to collect XANES and EXAFS spectra as the monochromator travels both up and down in energy (Khalid et al., 2010). Combined with electronics that collect 2000 data points per second, this unique setup allows the collection of a single EXAFS scan in as little as 100 ms. Ginder-Vogel et al. (2009) and Landrot et al. (2009) used this beamline to examine the kinetics of Cr(III) and As(III) oxidation by HMO using XANES spectroscopy at sub-second time scales. For examples, using Q-XAS, As(III) and As(V) concentrations were determined every 0.98 s in batch reactions. The initial apparent As(III) depletion rate constants (t<30 s) measured with Q-XAS are nearly twice as large as rate constants measured with traditional analytical techniques (Ginder-Vogel et al., 2009). Landrot et al. (2010) determined the chemical (i.e., independent of physical phenomena) kinetics of Cr(III) oxidation. These results demonstrate the importance of developing analytical techniques capable of analyzing environmental reactions on the same time scale as they occur.

5. FUTURE NEEDS

As our knowledge of environmental systems continues to advance, it is critical that X-ray spectroscopic techniques continue advancing with the field. Currently, a primary limitation of the application of X-ray techniques to environmental systems is the availability of adequate amounts of beamtime. This problem can be resolved by advances in both user support and instrumentation. Several improvements in user administration and services, including standardized data collection software, state-of-the-art data analysis software, increased beamline support staff, and improvements in laboratory support facilities, would allow for the more efficient use of limited beamtime. The heterogeneity of environmental samples requires both the application of a wide array of techniques, including X-ray spectroscopic and traditional ones, and more time using each individual technique. The enhanced intensity and flux of third generation synchrotron light sources allow for the analysis of both lower concentration elements and smaller samples; however, many environmental samples also require a broad energy range (5-50 keV), high-energy resolution (0.1 eV), and a range of spatial resolutions (bulk, micro, and nano). Additionally, unique end-station capabilities, including flow-through reaction cells and anaerobic gloveboxes, coupled with fast-scanning, high-energy resolution fluorescent detection and simultaneous collection of XRD and XAS data, will take advantage of the unique ability of X-ray absorption to analyze samples *in situ*, allowing a new generation of complex environmental problems to be solved.

ACKNOWLEDGMENTS

The authors would like to acknowledge funding from the NSF EPSCoR Program, grant #EPS-0447610. A portion of this work was conducted at Stanford Synchrotron Radiation Laboratory, a national user facility operated by Stanford University on behalf of the US Department of Energy, Office of Basic Energy Sciences. The SSRL Structural Molecular Biology Program is supported by the Department of Energy, Office of Biological and Environmental Research, and by the National Institutes of Health, National Center for Research Resources, Biomedical Technology Program. A portion of this work was performed at GeoSoilEnviroCARS (Sector 13), Advanced Photon Source (APS), and Argonne National Laboratory. GeoSoilEnviroCARS is supported by the National Science Foundation—Earth Sciences (EAR-0622171) and Department of Energy—Geosciences (DE-FG02-94ER14466). Use of the Advanced Photon Source was supported by the US Department of Energy, Office of Science, Office of Basic Energy Sciences, under Contract No. DE-AC02-06CH11357. Use of the National Synchrotron Light Source, Brookhaven National Laboratory, was supported by the US Department of Energy, Office of Science, Office of Basic Energy Sciences, under Contract No. DE-AC02-98CH10886. The Advanced Light Source is supported by the Director, Office of Science, Office of Basic Energy Sciences, of the U.S. Department of Energy under Contract No. DE-AC02-05CH11231.

References

Allmann, R., 1970. Double layer structures with layer ions $[Me(II)_{1-x} Me(III)_x (OH)_2]^{x+}$ of brucite type. Chimia 24, 99–108.

Arai, Y., Lanzirotti, A., Sutton, S.R., Newville, M., Dyer, J., Sparks, D.L., 2006. Spatial and temporal variability of arsenic solid-state speciation in historically lead arsenate contaminated soils. Environ. Sci. Technol. 40, 673–679.

Bank, T.L., Vishnivetskaya, T.A., Jardine, P.M., Ginder-Vogel, M.A., Fendorf, S., Baldwin, M.E., 2007. Elucidating biogeochemical reduction of chromate via carbon amendments and soil sterilization. Geomicrobiol. J. 24, 125–132.

Bargar, J.R., Brown, G.E., Parks, G.A., 1995. XAFS study of Pb(II) sorption at the a-Al_2O_3-water interface. Physica B 209, 455–456.

Beauchemin, S., Hesterberg, D., Chou, M., Beauchemin, R., Simard, R., Sayers, D.E., 2003. Speciation of phosphorus in P-enriched agricultural soils using XANES spectroscopy and chemical fractionation. J. Environ. Qual. 32, 1809–1819.

Bertsch, P.M., Hunter, D.B., 1998. Elucidating fundamental mechanisms in soil and environmental chemistry: the role of advanced analytical, spectroscopic, and microscopic methods. In: Huang, P.M. (Ed.), Future Prospects for Soil Chemistry, vol. SSSA Spec. Pub. No. 55. Soil Sci. Soc. Am., Madison, WI, pp. 103–122.

Bertsch, P.M., Hunter, D.B., 2001. Applications of synchrotron-based X-ray microprobes. Chem. Rev. 101, 1809–1842.

Bertsch, P.M., Seaman, J.C., 1999. Characterization of complex mineral assemblages: implications for contaminant transport and environmental remediation. Proc. Natl. Acad. Sci. U.S.A. 96, 3350–3357.

Bleam, W.F., 1991. Soil science applications of nuclear-magnetic-resonance spectroscopy. Adv. Agron. 46, 91–155.

Bostick, B.C., Doyle, C., Fendorf, S., Kendelewicz, T., Bargar, J., Brown, G.E., 2002. Role of arsenic in pyrite oxidation. Geochim. Cosmochim. Acta 66, A95.

Brown, G., Parks, G., 2001. Sorption of trace elements on mineral surfaces: modern perspectives from spectroscopic studies, and comments on sorption in the marine environment. Int. Geol. Rev. 43, 963–1073.

Brown G.E. Jr., Sturchio, N.C., 2002. An overview of synchrotron radiation applications to low temperature geochemistry and environmental science. In: Fenter, P.A., Rivers, M.L., Sturchio, N.C., Sutton, S.R. (Eds.), Applications of Synchrotron Radiation in Low-Temperature Geochemistry and Environmental Sciences. Geochem. Soc., Mineral. Soc. Am., Washington, DC, pp. 1–115.

Brown, G.E., Bargar, J.R., Towle, S.N., 1997a. Use of X-ray absorption spectroscopy to study reaction mechanisms at oxide-water interfaces. Abstr. Pap. Am. Chem. Soc. 213, 36-Geoc.

Brown, G.E., Foster, A., Ostergren, J., Bargar, J.R., 1997b. X-ray absorption spectroscopy and molecular environmental science. Abstr. Pap. Am. Chem. Soc. 214, 10-Geoc.

Brown, G.E., Calas, G., Hemley, R.J., 2006. Scientific advances made possible by user facilities. Elements 2, 23–30.

Buswell, A.M., Krebs, K., Rodebush, W.H., 1937. Infrared studies. III. Absorption bands of hydrogels between 2.5 and 3.5 m. J. Am. Chem. Soc. 59, 2603–2605.

Cail, T.L., Hochella, M.F., 2005. Experimentally derived sticking efficiencies of microparticles using atomic force microscopy. Environ. Sci. Technol. 39, 1011–1017.

Catalano, J.G., Park, C., Fenter, P., Zhang, Z., 2008. Simultaneous inner- and outer-sphere arsenate adsorption on corundum and hematite. Geochim. Cosmochim. Acta 72, 1986–2004.

Charlet, L., Manceau, A., 1992. X-ray absorption spectroscopic study of the sorption of Cr(III) at the oxide-water interface. II: adsorption, coprecipitation and surface precipitation on ferric hydrous oxides. J. Colloid Interface Sci. 148, 443–458.

Chen, Q., Kinzelbach, W., Oswald, S., 2002a. Nuclear magnetic resonance imaging for studies of flow and transport in porous media. J. Environ. Qual. 31, 477–486.

Chen, Q., Kinzelbach, W., Ye, C., Yue, Y., 2002b. Variations of permeability and pore size distribution of porous media with pressure. J. Environ. Qual. 31, 500–505.

Chisholm-Brause, C.J., O'Day, P.A., Brown G.E. Jr., Parks, G.A., 1990. Evidence for multinuclear metal-ion complexes at solid/water interfaces from X-ray absorption spectroscopy. Nature 348, 528–530.

Chisholm-Brause, C.J., Conradson, S.D., Buscher, C.T., Eller, P.G., Morris, D.E., 1994. Speciation of uranyl sorbed at multiple binding sites on montmorillonite. Geochim. Cosmochim. Acta 58, 3625–3631.

Dent, A.J., 2002. Development of time-resolved XAFS instrumentation for quick EXAFS and energy-dispersive EXAFS measurements on catalyst systems. Top. Catal. 18, 27–35.

Elzinga, E.J., Sparks, D.L., 1999. Nickel sorption mechanisms in a pyrophyllite-montmorillonite mixture. J. Colloid Interface Sci. 213, 506–512.

Elzinga, E.J., Sparks, D.L., 2001. Reaction condition effects on nickel sorption mechanisms in illite-water suspensions. Soil Sci. Soc. Am. J. 65, 94–101.

EnviroSuite, 2008. EnviroSuite: a unified voice for molecular environmental science at BNL.

Farley, K.J., Dzombak, D.A., Morel, F.M.M., 1985. A surface precipitation model for the sorption of cations on metal oxides. J. Colloid Interface Sci. 106, 226–242.

Fendorf, S.E., 1999. Fundamental aspects and applications of X-ray absorption spectroscopy in clay and soil science. In: Schulze, D.G., Stucki, J.W., Bertsch, P.M. (Eds.), Synchrotron X-ray Methods in Clay Science. Clay Miner. Soc., Boulder, Colorado, pp. 20–67.

Fendorf, S.E., Zasoski, R.J., 1992. Chromium(III) oxidation by delta-MnO_2. Environ. Sci. Technol. 26, 79–85.

Fendorf, S.E., Fendorf, M., Sparks, D.L., Gronsky, R., 1992. Inhibitory mechanisms of Cr(III) oxidation by d-MnO_2. J. Colloid Interface Sci. 153, 37–54.

Fendorf, S.E., Sparks, D.L., Franz, J.A., Camaioni, D.M., 1993. Electron paramagnetic resonance stopped-flow kinetic study of manganese (II) sorption-desorption on birnessite. Soil Sci. Soc. Am. J. 57, 57–62.

Fendorf, S., Lamble, G., Stapleton, M.G., Kelley, M.J., Sparks, D.L., 1994. Mechanisms of chromium(III) soprtion on silica. 1. Cr(III) surface structure derived by extended X-ray absorption fine structure spectroscopy. Environ. Sci. Technol. 28, 284–289.

Fendorf, S., Hansel, C.M., Wielinga, B.W., 2002. Operative pathways of chromate and uranyl reduction within soils and sediments. In: Zhang, P.-C., Brady, P.V. (Eds.), Geochemistry of Soil Radionuclides, vol. Special Publication No. 59. Soil Sci. Soc. Am. Madison, WI.

Fenter, P.A., River, M.L., Sturchio, N.C., Sutton, S.R., 2002. Applications of synchrotron radiation in low-temperature geochemistry and environmental science. Mineral. Soc. Am., Washington, DC.

Flogeac, K., Guillon, E., Aplincourt, M., 2004. Surface complexation of copper(II) on soil particles: EPR and XAFS studies. Environ. Sci. Technol. 38, 3098–3103.

Ford, R.G., Sparks, D.L., 2000. The nature of Zn precipitates formed in the presence of pyrophyllite. Environ. Sci. Technol. 34, 2479–2483.

Ford, R.G., Scheinost, A.C., Scheckel, K.G., Sparks, D.L., 1999. The link between clay mineral weathering and the stabilization of Ni surface precipitates. Environ. Sci. Technol. 33, 3140–3144.

Fredrickson, J.K., Zachara, J.M., Kennedy, D.W., Dong, H.L., Onstott, T.C., Hinman, N.W., et al., 1998. Biogenic iron mineralization accompanying the dissimilatory reduction of hydrous ferric oxide by a groundwater bacterium. Geochim. Cosmochim. Acta 62, 3239–3257.

GeoSoilEnviroCARS, 2008. GSECARS Home Page.

Ghosal, S., Hemminger, J.C., Bluhm, H., Mun, B.S., Hebenstreit, E.L.D., Ketteler, G., et al., 2005. Electron spectroscopy of aqueous solution interfaces reveals surface enhancement of halides. Science 307, 563–566.

Ginder-Vogel, M., Fendorf, S., 2008. Biogeochemical uranium redox transformation: potential oxidants of uraninite. In: Barnett, M.O., Kent, D.B. (Eds.), Adsorption of Metals by Geomedia II: Variables, Mechanisms, and Model Applications, vol. 7. Elsevier, Amsterdam, The Netherlands, pp. 293–320.

Ginder-Vogel, M., Stewart, B., Fendorf, S., 2010. Kinetic and mechanistic constraints on the oxidation of biogenic uraninite by ferrihydrite. Environ. Sci. Technol. 44, 163–169.

Ginder-Vogel, M., Borch, T., Mayes, M.A., Jardine, P.M., Fendorf, S., 2005. Chromate reduction and retention processes within arid subsurface environments. Environ. Sci. Technol. 39, 7833–7839.

Ginder-Vogel, M., Criddle, C., Fendorf, S., 2006. Thermodynamic constraints on the oxidation of biogenic UO_2 by Fe(III) (hydr)oxides. Environ. Sci. Technol. 40, 3544–3550.

Ginder-Vogel, M., Landrot, G., Fischel, J.S., Sparks, D.L., 2009. Quantification of rapid environmental redox processes with quick-scanning X-ray absorption spectroscopy (Q-XAS). Proc. Natl. Acad. Sci. U.S.A. 106, 16124–16128.

Grafe, M., Tappero, R.V., Marcus, M.A., Sparks, D.L., 2008. Arsenic speciation in multiple metal environments - II. Micro-spectroscopic investigation of a CCA contaminated soil. J. Colloid Interface Sci. 321, 1–20.

Hansel, C.M., Benner, S.G., Neiss, J., Dohnalkova, A., Kukkadapu, R.K., Fendorf, S., 2003a. Secondary mineralization pathways induced by dissimilatory iron reduction of ferrihydrite under advective flow. Geochim. Cosmochim. Acta 67, 2977–2992.

Hansel, C.M., Wielinga, B.W., Fendorf, S., 2003b. Structural and compositional evolution of Cr/Fe solids after indirect chromate reduction by dissimilatory iron-reducing bacteria. Geochim. Cosmochim. Acta 67, 401–412.

Hansel, C.M., Benner, S.G., Fendorf, S., 2005. Competing Fe (II)-induced mineralization pathways of ferrihydrite. Environ. Sci. Technol. 39, 7147–7153.

Hayes, K.F., Roe, A.L., Brown G.E. Jr., Hodgson, K.O., Leckie, J.O., Parks, G.A., 1987. *In situ* X-ray absorption study of surface complexes: selenium oxyanions on a-FeOOH. Science 238, 783–786.

Hesterberg, D., Zhou, W., Hutchinson, K.J., Beauchemin, S., 1999. XAFS study of adsorbed and mineral forms of phosphate. J. Synchrotron Radiat. 6, 636–638.

Hillner, P.E., Manne, S., Gratz, A.J., Hansma, P.K., 1992. AFM images of dissolution and growth on a calcite crystal. Ultramicroscopy 44, 1387–1393.

Hind, A.R., Bhargava, S.K., McKinnon, A., 2001. At the solid/liquid interface: FTIR/ATR—the tool of choice. Adv. Colloid Interface Sci. 93, 91–114.

Hunter, D.B., Bertsch, P.M., 1998. *In situ* examination of uranium contaminated soil particles by micro-X-ray absorption and micro-fluorescence spectroscopies. J. Radioanal. Nucl. Chem. 234, 237–242.

Isaure, M.P., Laboudigue, A., Manceau, A., Sarret, G., Tiffreau, C., Trocellier, P., et al., 2002. Quantitative Zn speciation in a contaminated dredged sediment by m-PIXE; m-SXRF; EXAFS spectroscopy and principal component analysis. Geochim. Cosmochim. Acta 66, 1549–1567.

Johnston, C.T., Wang, S.-L., 2002. Applications of vibrational spectroscopy in soil and environmental sciences. In: Chalmers, J.M., Griffithins, P.R. (Eds.), Handbook of Vibrational Spectroscopy, vol. 4. John Wiley & Sons Ltd, West Sussex, UK, pp. 3192–3205.

Kelly, S.D., Kemner, K.M., Fein, J.B., Fowle, D.A., Boyanov, M.I., Bunker, B.A., et al., 2002. X-ray absorption fine structure determination of pH-dependent U-bacterial cell wall interactions. Geochim. Cosmochim. Acta 66, 3855–3871.

Kelly, S.D., Kemner, K.M., Brooks, S.C., 2007. X-ray absorption spectroscopy identifies calcium-oranyl-carbonate complexes at environmental concentrations. Geochim. Cosmochim. Acta 71, 821–834.

Kelly, S.D., Hesterberg, D., Ravel, B., 2008. Analysis of soils and minerals using X-ray absorption spectroscopy. In: Ulery, A.L., Drees, L.R. (Eds.), Methods of Soil Analysis Part 5: Mineralogical Methods, vol. 5. Soil Sci. Soc. Am., Inc., Madison, Wisconsin, USA.

Kendelewicz, T., Liu, P., Doyle, C.S., Brown, G.E., 2000. Spectroscopic study of the reaction of aqueous Cr(VI) with Fe_3O_4(111) surfaces. Surf. Sci. 469, 144–163.

Khalid, S., Caliebe, W., Siddons, P., So, I., Clay, B., Lenhard, T., et al., 2010. Quick extended x-ray absorption fine structure instrument with millisecond time scale, optimized for *in situ* applications. Rev Sci. Instrum. 81, 015105.

Kinchesh, P., Samoilenko, A.A., Preston, A.R., Randall, E.W., 2002. Stray field nuclear magnetic resonance of soil water: development of a new, large probe and preliminary results. J. Environ. Qual. 31, 494–499.

Kocar, B.D., Herbel, M.J., Tufano, K.J., Fendorf, S., 2006. Contrasting effects of dissimilatory iron(III) and arsenic (V) reduction on arsenic retention and transport. Environ. Sci. Technol. 40, 6715–6721.

Landrot, G., Ginder-Vogel, M., Sparks, D.L., 2010. Kinetics of Chromium(III) Oxidation by Manganese(IV) Oxides Using Quick Scanning X-ray Absorption Fine Structure Spectroscopy (Q-XAFS). Environ. Sci. Technol. 44, 143–149.

Liu, C.G., Zachara, J.M., Gorby, Y.A., Szecsody, J.E., Brown, C.F., 2001. Microbial reduction of Fe(III) and sorption/precipitation of Fe(II) on *Shewanella putrefaciens* strain CN32. Environ. Sci. Technol. 35, 1385–1393.

Livi, K.J.T., Senesi, G.S., Scheinost, A.C., Sparks, D.L., 2009. Microscopic examination of nanosized mixed Ni-Al hydroxide surface precipitates on pyrophyllite. Environ. Sci. Technol. 43, 1299–1304.

Manceau, A., Charlet, L., 1994. The mechanism of selenate adsorption on goethite and hydrous ferric oxide. J. Colloid Interface Sci. 164, 87–93.

Manceau, A., Lanson, B., Schlegel, M.L., Harge, J.C., Musso, M., Eybert-Berard, L., et al., 2000. Quantitative Zn speciation in smelter-contaminated soils by EXAFS spectroscopy. Am. J. Sci. 300, 289–343.

Manceau, A., Marcus, M.A., Tamura, N., Proux, O., Geoffroy, N., Lanson, B., 2003. Natural speciation of Zn at the micrometer scale in a clayey soil using X-ray fluorescence, absorption, and diffraction. Geochim. Cosmochim. Acta 68, 2467–2483.

Manning, B.A., Fendorf, S.E., Bostick, B., Suarez, D.L., 2002. Arsenite(III) oxidation and arsenic(V) adsorption reactions on synthetic birnessite. Environ. Sci. Technol. 36, 976–981.

McBride, M.B., 1991. Processes of heavy and transition metal sorption by soil minerals. In: Bolt, G.H., Boodt, M.F.D., Hayes, M.H.B., McBride, M.B. (Eds.), Interactions at the Soil Colloid-Soil Solution Interface, vol. 190. Kluwer Academic Publishers, Dordrecht, pp. 149–176.

McBride, M.B., 1994. Environmental Chemistry of Soils. Oxford University Press, New York.

Mc Cammon, C.A., 2004. Mössbauer spectroscopy: applications. In: Beran, A., Libowitzky, E. (Eds.), Spectroscopic Methods in Mineralogy, vol. 6. Eur. Mineral. Soc., Vienna, Austria, pp. 369–398.

McNear D.H. Jr., Tappero, R., Sparks, D.L., 2005. Shining light on metals in the environment. Elements 1, 211–216.

McNear, D.H., Chaney, R.L., Sparks, D.L., 2007. The effects of soil type and chemical treatment on nickel speciation in refinery enriched soils: a multi-technique investigation. Geochim. Cosmochim. Acta 71, 2190.

MEIS, 2008. Molecular environmental and interface science at SSRL.

Mitsunobu, S., Takahashi, Y., Uruga, T., 2006. Observation of chemical reactions at the solid-water interface by quick XAFS combined with a column reactor. Anal. Chem. 78, 7040–7043.

Murad, E., Cashion, J., 2003. Mossbauer Spectroscopy of Environmental Materials and their Industrial Utilization. Kluwer Academic Publishers, Norwell, MA.

Nachtegaal, M., Marcus, M.A., Sonke, J.E., Vangronsveld, J., Livi, K.J.T., Van der Lelie, D., et al., 2005. Effects of *in situ* remediation on the speciation and bioavailability of zinc in a smelter contaminated soil. Geochim. Cosmochim. Acta 69, 4649–4664.

Nanny, M.A., Minear, R.A., Leenheer, J.A., 1997. Nuclear Magnetic Resonance Spectroscopy in Environmental Chemistry. Oxford Press, New York.

Nico, P.S., Stewart, B.D., Fendorf, S., 2010. Incorporation of oxidized uranium into Fe (Hydr) oxides during Fe(II) catalyzed remineralization. Environ. Sci. Technol. 43, 7391–7396.

O'Day, P.A., Brown, G.E., Parks, G.A., 1994. X-ray absorption spectroscopy of cobalt (II) multinuclear surface complexes and surface precipitates on kaolinite. J. Colloid Interface Sci. 165, 269–289.

Papelis, C., Hayes, K.F., 1996. Distinguishing between interlayer and external sorption sites of clay minerals using X-ray absorption spectroscopy. Colloids Surf. 107, 89.

Parikh, S.J., Lafferty, B.J., Sparks, D.L., 2008. An ATR-FTIR spectroscopic approach for measuring rapid kinetics at the mineral/water interface. J. Colloid Interface Sci. 320, 177–185.

Patterson, R.R., Fendorf, S., Fendorf, M., 1997. Reduction of hexavalent chromium by amorphous iron sulfides. Environ. Sci. Technol. 31, 2039–2044.

Paul, K.W., Kubicki, J.D., Sparks, D.L., 2007. Sulphate adsorption at the Fe (hydr)oxide-H_2

Sposito, G., 1986. Distinguishing adsorption from surface precipitation. In: Davis, J.A., Hayes, K.F. (Eds.), Geochemical Processes at Mineral Surfaces, vol. 323. Am. Chem. Soc., Washington, DC, pp. 217–229.

Stewart, B.D., Nico, P.S., Fendorf, S., 2009. Stability of uranium incorporated into Fe (Hydr)oxides under fluctuating redox conditions. Environ. Sci. Technol. 43, 4922–4927.

Strawn, D.G., Sparks, D.L., 1999. The use of XAFS to distinguish between inner- and outer-sphere lead adsorption complexes on montmorillonite. J. Colloid Interface Sci. 216, 257–269.

Strawn, D.G., Doner, H.E., Zavarin, M., McHugo, S.A., 2002. Microscale investigation in to the geochemistry of arsenic, selenium and iron in soil developed in pyritic shale materials. Geoderma 108, 237–257.

Sutton, S.R., 2006. User research facilities in the earth sciences. Elements. 2, 7–8.

Taylor, R.M., 1984. The rapid formation of crystalline double hydroxy salts and other compounds by controlled hydrolysis. Clay Miner. 19, 591–603.

Thompson, H.A., Parks, G.A., Brown, G.E., 1999a. Ambient-temperature synthesis, evolution, and characterization of cobalt-aluminum hydrotalcite-like solids. Clays Clay Miner. 47, 425–438.

Thompson, H.A., Parks, G.A., Brown, G.E., 1999b. Dynamic interactions of dissolution, surface adsorption, and precipitation in an aging cobalt(II)-clay-water system. Geochim. Cosmochim. Acta 63, 1767–1779.

Toor, G.S., Cade-Menun, B.J., Sims, J.T., 2005. Establishing a linkage between phosphorus forms in dairy diets, feces, and manures. J. Environ. Qual. 34, 1380–1391.

Towle, S.N., Bargar, J.R., Brown G.E. Jr, Parks, G.A., 1997. Surface precipitation of Co(II) (aq) on Al_2O_3. J. Colloid Interface Sci. 187, 62–82.

Weaver, R.M., Hochella M.F. Jr, 2003. The reactivity of seven Mn-oxides with Cr^{3+}aq: a comparative analysis of a complex, environmentally important redox reaction. Am. Mineral. 88, 2016–2027.

Webb, S.M., Bargar, J.R., Tebo, B.M., 2005a. Determination of uranyl incorporation into biogenic manganese oxides using X-ray absorption spectroscopy and scattering. Phys. Scripta T115, 949–952.

Webb, S.M., Tebo, B.M., Bargar, J.R., 2005b. Structural characterization of biogenic Mn oxides produced in seawater by the marine *bacillus sp.* strain SG-1. Am. Mineral. 90, 1342–1357.

Williams, A.G.B., Scherer, M.M., 2004. Spectroscopic Evidence for Fe(II)-Fe(III) electron transfer at the iron oxide-water interface. Environ. Sci. Technol. 38, 4782–4790.

Zhang, P.C., Sparks, D.L., 1990. Kinetics and mechanisms of sulfate adsorption desorption on goethite using pressure-jump relaxation. Soil Sci. Soc. Am. J. 54, 1266–1273.